

Space Weather®



RESEARCH ARTICLE

10.1029/2023SW003656

Key Points:

- The first scintillation event has larger maximum S₄ values and longer mean duration when compared to the subsequent events
- The durations of the scintillation events decrease with local time. The spacing between consecutive events shows the opposite trend; and
- Earlier occurrences of onset times are related to the increased probability of the occurrence of multiple scintillation events

Correspondence to:

A. Moraes, aom@ita.br

Citation:

Moraes, A., Sousasantos, J., Costa, E., Pereira, B. A., Rodrigues, F., & Galera Monico, J. F. (2024). Characterization of scintillation events with basis on L1 transmissions from geostationary SBAS satellites. *Space Weather*, 22, e2023SW003656. https://doi. org/10.1029/2023SW003656

Received 26 JUL 2023 Accepted 22 DEC 2023

Author Contributions:

Conceptualization: Alison Moraes, Emanoel Costa

Data curation: João Francisco Galera Monico

Formal analysis: Alison Moraes, Jonas Sousasantos, Bruno Augusto Pereira Funding acquisition: João Francisco Galera Monico

Investigation: Alison Moraes, Jonas Sousasantos, Bruno Augusto Pereira Methodology: Alison Moraes, Jonas Sousasantos, Bruno Augusto Pereira, Fabiano Rodrigues

Project Administration: João Francisco Galera Monico

Supervision: João Francisco Galera Monico

Validation: Bruno Augusto Pereira Visualization: Bruno Augusto Pereira

© 2024. The Authors.

This is an open access article under the terms of the Creative Commons Attribution License, which permits use, distribution and reproduction in any medium, provided the original work is properly cited.

Characterization of Scintillation Events With Basis on L1 Transmissions From Geostationary SBAS Satellites

Alison Moraes¹, Jonas Sousasantos², Emanoel Costa³, Bruno Augusto Pereira⁴, Fabiano Rodrigues², and João Francisco Galera Monico⁵

¹Instituto de Aeronáutica e Espaço—IAE, São José dos Campos, Brazil, ²William B. Hanson Center for Space Sciences, University of Texas at Dallas—UT Dallas, Richardson, TX, USA, ³Centro de Estudos em Telecomunicações, Pontifícia Universidade Católica do Rio de Janeiro (CETUC/PUC-Rio), Rio de Janeiro, Brazil, ⁴Instituto Tecnológico de Aeronáutica—ITA, São José dos Campos, Brazil, ⁵Universidade Estadual Paulista Júlio de Mesquita Filho—UNESP, Presidente Prudente, Brazil

Abstract Signals recorded by two stations in the Brazilian region: [Fortaleza (3.74°S, 38.57°W) and Inconfidentes (22.31°S, 46.32°W)], receiving L1 transmissions from different geostationary satellites, were used to evaluate the amplitude scintillation index S_4 and several characteristics of scintillation events (continuous record with $S_4 > 0.2$) during nighttime hours (18:00 LT–02:00 LT) in the years 2014–2016. The effects from solar activity, season, and local time on the number of scintillation events per night, maximum scintillation, scintillation event duration, and spacing between consecutive events will be discussed. The results indicate that: (a) scintillation occurs from September to March in both links; (b) the most likely numbers of observed scintillation events per night were two or three, particularly during the first 2 years; (c) on average, the first scintillation event usually had larger maximum S_4 values when compared to those of the later ones along the night; (d) the first scintillation event had a longer mean duration than the succeeding ones in a given night; (e) the durations of scintillation events, regardless of their numbers per night and the location, decreased with local time; (f) the opposite dependence of spacings between consecutive events on local time was observed; (g) the cumulative distribution functions of the scintillation onset time indicated a strong dependence on the dip latitude of the station; and (h) early occurrences of onset times are directly related to the increased probability of the occurrence of multiple scintillation events.

Plain Language Summary This study used radio signals from geostationary satellites collected from two ground-based stations in distinct dip latitudes over Brazil to evaluate aspects of amplitude scintillation. The investigation focused on the number of occurrences and in their specific characteristics such as intensity, duration, and spacing between consecutive scintillation events. The early nighttime hours, when scintillation is more likely to affect the signals were considered during the months of September to March over the years of 2014–2016, covering varied seasonal and solar flux conditions. The findings indicate that scintillation events earlier in the night have larger S_4 values and longer duration, being more severe for transionospheric signals. The results also show that earlier onset of scintillation events is likely to indicate multiple events over the night. These new findings contribute to the understanding of scintillation phenomenon and provide valuable insights for improving satellite-based systems in equatorial and low-latitude regions.

1. Introduction

A wide range of services and applications, such as precision agriculture, telecommunications, and ground, maritime, and air transportation systems, rely on Global Navigation Satellite System (GNSS) information. These applications have different reliability and safety requirements, but all depend on GNSS accuracy to successfully operate. However, in equatorial and low latitudes, ionospheric phenomena, including Equatorial Plasma Bubbles (EPBs), ionospheric scintillation, and the Equatorial Ionization Anomaly (EIA), very often hinder these requirements and compromise the operations of these systems (Moraes, Vani, et al., 2018; Sousasantos et al., 2021; Vani et al., 2019, 2021).

Ionospheric scintillation is experienced by radio signals that intersect EPBs, which are regions of plasma density depletions generated as a result from the so-called generalized Rayleigh-Taylor instability, that find favorable growth conditions during nighttime in the geomagnetic equator region (Dungey, 1956; Kelley, 1989; and references therein). Within EPBs, plasma density irregularities with scale sizes ranging from hundreds of kilometers

MORAES ET AL. 1 of 17

Writing – original draft: Alison Moraes, Jonas Sousasantos, Emanoel Costa Writing – review & editing: Emanoel Costa, Fabiano Rodrigues, João Francisco Galera Monico to tens of meters are created by secondary plasma instabilities. Irregularities with scale sizes of hundreds of meters are responsible for ionospheric scintillation in the *L* frequency band, from 1 to 2 GHz (Yeh & Liu, 1982). Consequently, during EPB events, systems based on GNSS may be severely affected, due to abnormal ionospheric delay errors and signal fading.

During the peak and moderate sections of the solar cycle, EPBs may rise with large velocities, reaching high apex altitudes, immediately above the geomagnetic equator (Dabas & Reddy, 1990). Due to geomagnetic-field alignment, this upward motion is accompanied by an increase in the EPB latitudinal extent (Whalen, 2000). Results from numerical simulation modeling, based on fundamental laws of ionospheric electrodynamics, show that, in addition to the above behavior, complex structuring processes (that could lead to bifurcation and merging) are more likely to be observed at the top of the EPBs (Huba et al., 2015; Keskinen et al., 1998; Yokoyama, 2017). Studies of EPB characteristics were also developed with basis on in situ and ground-based experimental data (Burke et al., 2004a, 2004b; Costa et al., 2018; Gentile et al., 2011; Huang et al., 2014; Kil & Heelis, 1998; Sobral et al., 2002; Takahashi et al., 2015). Modeling and experimental studies of EPB characteristics complement each other.

Of relevance to the current study, Roddy et al. (2010) presented a comparison of in situ ion density fluctuations measured by the Planar Langmuir Probe (PLP) onboard the Communication/Navigation Outage Forecasting System (C/NOFS) satellite with coincident ground-based scintillation measurements from the Scintillation Decision Aid network and coherent-scatter radar located on Christmas Island (3°N, 157°W) over a 15-month period. They concluded that, as a broad predictive tool, in situ measurements of structure in the ionosphere were promising in nowcasting scintillation. Adapting this approach, Costa et al. (2020) applied a modified version of a weak-scatter scintillation model to propagation paths between an Earth station and two geostationary satellites, as they are affected by drifting ionospheric irregularities detected by the PLP onboard the C/NOFS satellite, to analyze scintillation and space-diversity mitigation effects on it.

Shume et al. (2013) applied the wavelet decomposition technique to flux tubes in the Brazilian and Pacific sectors to show that dominant density irregularities associated with the rapidly changing amplitude scintillation oscillations displayed periods between 4 and 15 min. These periods match those of atmospheric gravity waves, prompting them to suggest that they might play a role in the generation of the rapidly changing scintillation-producing irregularities (or bifurcations). They also concluded that the scintillation-producing irregularities are anisotropic along flux tubes, as well as in the east-west direction. Finally, they stressed that understanding attributes of these irregularities is important for the development of measures to mitigate L-band scintillation effects on signals transmitted by communication and navigation satellites. Shume and Mannucci (2013), inspired by Caton and Groves (2006), applied a phase and coherence methodology to S_4 data from fixed transionospheric links with equatorial Ionospheric Pierce Points (IPPs) mutually separated between 21.3° and 23.4° in longitude. They concluded that, if L-band scintillation occurred in the eastern link, there was a 95% likelihood that scintillation would occur in the western link after 2–3 hr. This result suggests that the development of scintillation prediction system westward of observation sites is possible.

Understanding the dynamics of scintillation events and its dependence on the environment is crucial, as an aid to predictions of this phenomenon based on space weather conditions. Such characterization can also help minimizing scintillation impacts on GNSS-based applications, particularly those involved in critical ones such as air navigation.

The objective of this paper is to investigate several characteristics of L-Band GNSS amplitude scintillation events as experienced by signals from geostationary satellites. Therefore, it distinguishes itself and complements previous studies by directly using experimental scintillation data from fixed links defined by two Brazilian locations with different dip latitudes, each receiving L1 (1,575.42 MHz) signals from different geostationary satellites of the Space-Based Augmentation System (SBAS) under distinct solar activity, seasonal, and local-time conditions. Both receiving stations collected data during 3 years (2014–2016) in the maximum and descending phases of solar cycle 24. The results in this work advances knowledge on the characterization of scintillation events, directly presenting and discussing signal structures observed in GNSS transmissions and complementing information on radio wave propagation through EPBs previously reported in the literature. One of its distinguishing aspect is the utilization of fixed-link data (from geostationary satellites to ground monitors). Thus, the present investigation of the time evolution of scintillation events is entirely due to drifts of ionospheric structures across fixed paths. This time evolution of the received signal structures is not affected by satellite motions.

MORAES ET AL. 2 of 17

Table 1Station Coordinates and Specific Details of the Data Links Utilized in This Study

Parameter	Fortaleza	Inconfidentes	
Geographic Latitude	3.74°S	22.31°S	
Geographic Longitude	38.57°W	46.32°W	
Dip Latitude	7.64°S	18.95°S	
SBAS PRN (position)	136 (15.5°W)	120 (5.0°E)	
Azimuth	86°	58°	
Elevation	40°	47°	
IPP Latitude	3.50°S	20.87°S	
IPP Longitude	35.14°W	43.85°W	
IPP Dip Latitude	9.27°S	19.26°S	

The next sections are structured as follows. Section 2 provides details on the data used in the study and the methodologies adopted to define and determine the scintillation event characteristics of interest. Section 3 discusses the number of scintillation events observed per night and its seasonal behavior. Then, it addresses their intensities, durations, as well as spacings between consecutive ones, considering the number of events per night and local time, highlighting the variability of these structures. Finally, Section 4 summarizes the main findings of the paper with concluding remarks and lists future studies. In particular, it should be remarked that the study of precise relations between the analyzed characteristics of scintillation events and those of EPBs should also involve simultaneous additional in-situ or ground-based (radar or optical imaging) data, not available to the present work. Thus, references to characteristics of EPB structures in association to those of the analyzed scintillation events will only be made here in general and approximate terms.

2. Data Description and Scintillation Characteristics of Interest

As mentioned in the Introduction, scintillation in equatorial and low-latitude regions is caused by plasma irregularities associated with EPBs. Therefore,

scintillation in transionospheric radio signals can be used to investigate the effects from EPBs on radio wave propagation, some of its characteristics, as well as its impact on systems. The present study is based on the amplitude scintillation index S_4 , estimated as the standard deviation of $I/\langle I\rangle$, where I is the received signal intensity and $\langle ... \rangle$ represents an ensemble average (Yeh & Liu, 1982). The scintillation index S_4 was estimated from the data at every integer minute, using 3,000 intensity values sampled at 50 Hz.

The amplitude scintillation data were obtained between 01 January 2014 and 31 December 2016, during the maximum and decreasing phases of solar cycle 24. Approximately, the F10.7 index (solar radio flux at 10.7 cm, reported in solar flux units, where 1 sfu = 10^{-22} W·m⁻²·Hz⁻¹), one of the most widely used indices of solar activity, remained constant at 140 sfu during 2014 and linearly decreased in the intervals (140 sfu, 100 sfu) and (100 sfu, 80 sfu) during the respective years 2015 and 2016. In the present study, only data recorded during the period from 18:00 LT to 02:00 LT (21:00 UT to 05:00 UT) were considered. This time range was chosen to encompass the nighttime hours during which scintillation occurrence is the highest in the considered regions (e.g., Moraes, Muella, et al., 2018; Sousasantos et al., 2018).

The measurements were performed by two Septentrio PolaRx5S ground-based scintillation monitors, currently operated by the GNSS Technology to Support Air Navigation (GNSS NavAer) project, funded by the Brazilian Instituto Nacional de Ciência e Tecnologia (INCT). More details on the project can be found in Monico et al. (2022) and de Paula et al. (2023). The monitors were deployed at: (a) Fortaleza (close to the geomagnetic equator), receiving L1 transmissions from the EGNOS (European Geostationary Navigation Overlay Service) SBAS satellite Sirius-5 (PRN number 136, located at 5.0°E in the geostationary orbit); and (b) Inconfidentes (close to the southern crest of the EIA), receiving L1 transmissions from the EGNOS SBAS satellite Inmarsat I-3 F2 (PRN number 120, located at 15.5°W in the geostationary orbit). According to the discussion in the previous section, these two fixed links observe distinct ionospheric effects. The corresponding 350 km altitude IPPs were also assumed to remain fixed. Additional details regarding the two links and respective data are provided in Table 1. Hereafter, to simplify notation, the fixed links will only be identified by their ground stations (Fortaleza and Inconfidentes).

Figure 1 shows examples of scintillation records for the night between 09 and 10 November 2014, for Fortaleza (upper panel) and Inconfidentes (lower panel). The presence of EPBs intersecting the fixed SBAS links is represented by the increase in S_4 . Throughout the night, multiple EPB signatures were observed in the signals. When comparing the S_4 data from both stations, significant differences are noted in the numbers of detected structures, their respective durations and spacings, and strengths of the scintillation index S_4 .

To perform the analysis of the characteristics of scintillation events, this study employed the following criteria:

MORAES ET AL. 3 of 17

5427390, 2024, 1, Downloaded from https://agupubs.onlinelibrary.wiley.com/doi/10.1029/2023SW003656, Wiley Online Library on [07/07/2024]. See the Terms and Conditions (https://onlinelibrary.wiley.com/doi/10.1029/2023SW003656, Wiley Online Library on [07/07/2024]. See the Terms and Conditions (https://onlinelibrary.wiley.com/doi/10.1029/2023SW003656, Wiley Online Library on [07/07/2024]. See the Terms and Conditions (https://onlinelibrary.wiley.com/doi/10.1029/2023SW003656, Wiley Online Library on [07/07/2024]. See the Terms and Conditions (https://onlinelibrary.wiley.com/doi/10.1029/2023SW003656, Wiley Online Library on [07/07/2024]. See the Terms and Conditions (https://onlinelibrary.wiley.com/doi/10.1029/2023SW003656, Wiley Online Library on [07/07/2024]. See the Terms and Conditions (https://onlinelibrary.wiley.com/doi/10.1029/2023SW003656, Wiley Online Library on [07/07/2024]. See the Terms and Conditions (https://onlinelibrary.wiley.com/doi/10.1029/2023SW003656, Wiley Online Library on [07/07/2024]. See the Terms and Conditions (https://onlinelibrary.wiley.com/doi/10.1029/2023SW003656, Wiley Online Library on [07/07/2024]. See the Terms and Conditions (https://onlinelibrary.wiley.com/doi/10.1029/2023SW003656, Wiley Online Library on [07/07/2024]. See the Terms and Conditions (https://onlinelibrary.wiley.com/doi/10.1029/2023SW003656, Wiley Online Library on [07/07/2024]. See the Terms and Conditions (https://onlinelibrary.wiley.com/doi/10.1029/2023SW003656, Wiley Online Library.wiley.com/doi/10.1029/2023SW00366, Wiley Online Library.wiley.com/doi/10.1029/2023SW00366,

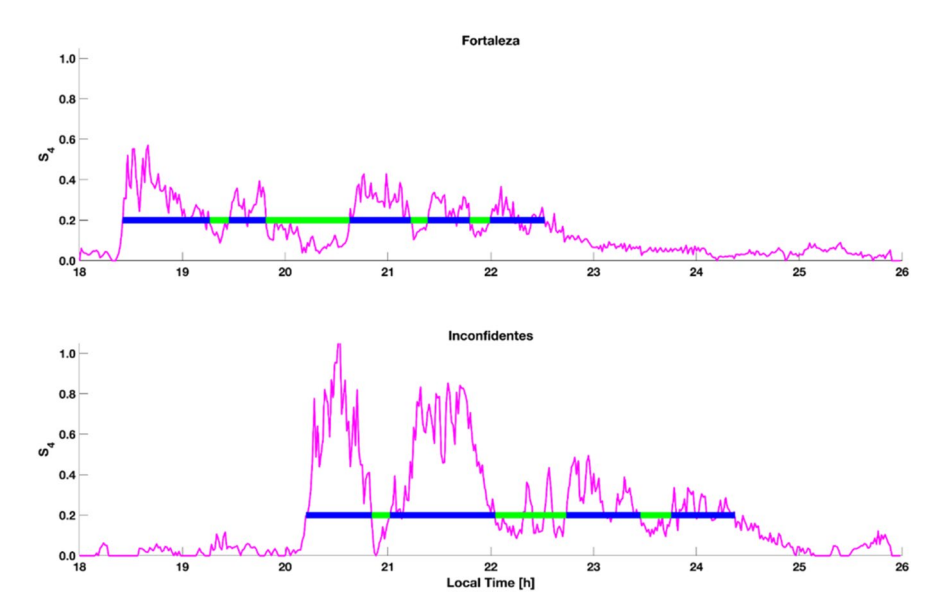


Figure 1. Examples of scintillation index (S_4) records of Space-Based Augmentation System signals received by the Fortaleza/Inconfidentes (upper/lower panels) monitors on the night between 09 and 10 November 2014. There are clear differences in the characteristics of the scintillation records corresponding to the two locations. Scintillation events, their durations and spacings are identified by thick blue and green horizontal segments at $S_4 = 0.2$, respectively.

- Each first sample of a continuous record with S₄ > 0.2 identifies the beginning time instant Ti of a scintillation
 event
- The same scintillation event ends at the time Tf of the first subsequent sample with $S_4 \le 0.2$.
- The duration of each scintillation event is computed as Tf Ti, if this difference is longer than 8 min. Cases with $S_4 > 0.2$ and durations shorter than 8 min (a "spike") are discarded from further analysis.
- The time interval between two consecutive scintillation events (spacing between them) is also computed.
- If the spacing between two consecutive scintillation events is shorter than 4 min, they are merged and the
 resulting duration is recalculated (Tf of the second case minus Ti of the first case).
- The maximum S_4 value between Ti and Tf for each scintillation event is also determined.

Scintillation events, their durations and spacings are identified in Figure 1 by thick blue and green horizontal segments at $S_4 = 0.2$, respectively. This threshold has been selected to be sufficiently low, but also to guarantee that the corresponding signal structures are essentially due to ionospheric effects, not being significantly contaminated by receiver noise (Muella et al., 2017; Sousasantos et al., 2018). The duration threshold Tf – Ti > 8 min, in combination with $S_4 > 0.2$, was adjusted to the data to discard a large number of short events ("spikes"), most of them with maximum S_4 value close to 0.2. Similarly, a minimum spacing (4 min, one half of the duration threshold) between consecutive scintillation events was imposed.

The total numbers of available nights and associated minutes; the numbers of nights with scintillation events and associated minutes; the number of events; and the numbers of minutes with $S_4 > 0.2$ and $S_4 > 0.7$ (strong scintillation) for the Fortaleza and Inconfidentes links and the years 2014–2016 are presented in Table 2. Nights with less than 180 min of data were discarded.

In Table 2, the eighth column also includes the number of minutes with $S_4 > 0.7$. Since data are collected at each site from 18:00 LT to 02:00 LT, the maximum number of samples per night is 480. Considering the total number of nights in the second column of Table 2, the total number of samples per station and year can be obtained. Dividing the available number of samples in the third column of Table 2 by the corresponding total number of samples, the following fractions are obtained: (a) Fortaleza (0.9704, 0.9864, 0.9873); (b) Inconfidentes (0.9926, 0.9958, 0.9851). A similar analysis involving the fourth and fifth columns provides the following fractions: (a) Fortaleza (0.9842, 0.9833, 0.9867); (b) Inconfidentes (0.9965, 0.9901, 0.9998). These fractions indicate that the selected data set has sufficient S_4 samples for investigating and detecting the scintillation events. For each night analyzed in this study, the number of scintillation events, their start (Ti) and end (Tf) times, durations, spacings

MORAES ET AL. 4 of 17



Space Weather

10.1029/2023SW003656

Table 2 Important Parameters of the Data Set										
Year	Total nights	Total minutes	Nights with events	Associated minutes	Number of events	Minutes $S_4 > 0.2$	Minutes $S_4 > 0.7$			
Fortaleza										
2014	184	85,705	94	44,407	280	12,040	132			
2015	256	121,209	120	56,638	381	14,769	50			
2016	245	116,109	62	29,365	183	7,604	21			
Inconfidentes										
2014	332	158,188	123	58,833	314	14,369	1,642			
2015	338	161,652	71	33,741	179	6,908	371			
2016	313	148,005	12	5,759	17	1,371	115			

and maximum S_4 values were stored for further analysis. The results will be presented and discussed in the next section.

3. Results and Discussion

The analysis investigated variations in scintillation event behavior as a function of solar activity, seasonal conditions, local time, and onset time for the two links (Fortaleza and Inconfidentes) being considered. Remember that Fortaleza and Inconfidentes are close to the geomagnetic equator and the southern crest of the EIA, respectively, thus providing observations under distinct geophysical regimes. Effects from changes in solar activity were investigated by considering data from sequential years (2014–2016), along which the F10.7 index experienced well-defined variations, characterized above.

3.1. Seasonal Dependence of the Number of Scintillation Events and Total Scintillation Time per Night

Initially, the seasonality aspect of the full data set will be discussed, to show how selected parameters of scintillation events vary throughout the year, considering nights with and without scintillation events. The total night numbers and corresponding minutes are shown in the second and third columns of Table 2.

The left/right panels in the upper row of Figure 2 show the number of available nights for each month of the 3 years in Fortaleza/Inconfidentes. The left/right panels in the middle row of Figure 2 show the mean number of scintillation events per night for each month of the 3 years in Fortaleza/Inconfidentes. The left/right panels in the lower row of Figure 2 do the same for the mean duration of scintillation events per night, displaying a considerable resemblance with those in the respective middle panels. The common horizontal axes of the 6 panels are segmented into 36 bins (1 bin for each month, from 01 January 2014 to 31 December 2016.

The data seasonality, evident in the two lower rows of Figure 2, is consistent with previous observations. Indeed, Stolle et al. (2008) indicated that the most striking features of their Equatorial Spread F (ESF) observations, consistently with earlier works in their reference list, were: (a) the very high occurrence rates of the phenomenon in the Brazilian/Atlantic sector during December solstice months; and (b) that this sector was almost void of events during June solstice months. In both links, scintillation occurs from September to March. Additionally, the values for the mean number of events and duration per night vary within the scintillation season. For example, the following observation are valid for both parameters and links: (a) the values associated with October or November tend to be larger than those associated with September and December; (b) for the clusters centered on January 2015 and January 2016, the values associated with February tend to be larger than those associated with January and March; and (c) the values associated with January 2014 or March 2014 generally exceed those associated with February 2014. These variations are supported by Akala et al. (2011), who also detected monthly variations in the occurrences and durations of events along the December Solstice and March Equinox in the high solar-activity period from November 2001 to October 2002 in Cuzco (14.0°S, 73.0°W, dip 1.0°S), Iquitos (3.8°S, 73.2°W, dip 7.0°N), and Bogota (4.4°N, 74.1°W, dip 16.0°N).

MORAES ET AL. 5 of 17

15427390, 2024, 1, Downloaded from https://agupubs.onlinelibrary.wiley.com/doi/10.1029/2023SW003656, Wiley Online Library on [07/07/2024]. See the Terms and Conditions (https://agupubs.onlinelibrary.wiley.com/ter/15427390, 2024, 1, Downloaded from https://agupubs.onlinelibrary.wiley.com/to/10.1029/2023SW003656, Wiley Online Library on [07/07/2024]. See the Terms and Conditions (https://agupubs.onlinelibrary.wiley.com/to/10.1029/2023SW003656, Wiley Online Library on [07/07/2024]. See the Terms and Conditions (https://agupubs.onlinelibrary.wiley.com/to/10.1029/2023SW003656, Wiley Online Library on [07/07/2024]. See the Terms and Conditions (https://agupubs.onlinelibrary.wiley.com/to/10.1029/2023SW003656, Wiley Online Library on [07/07/2024]. See the Terms and Conditions (https://agupubs.onlinelibrary.wiley.com/to/10.1029/2023SW003656, Wiley Online Library on [07/07/2024]. See the Terms and Conditions (https://agupubs.onlinelibrary.wiley.com/to/10.1029/2023SW003656, Wiley Online Library.wiley.com/to/10.1029/2023SW003656, Wile

and-conditions) on Wiley Online Library for rules of use; OA articles are governed by the applicable Creative Commons License

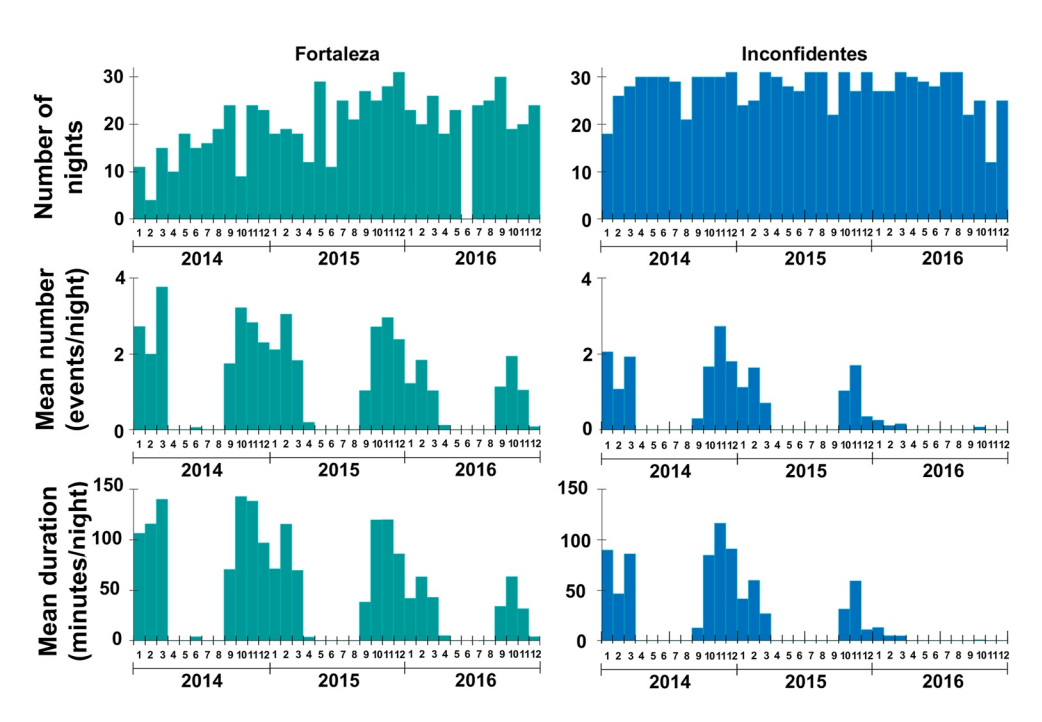


Figure 2. Upper-row panels: number of available nights from 01 January 2014 to 31 December 2016 in the Fortaleza/ Inconfidentes (left/right) links. Middle-row panels: mean number of scintillation events per night during the same period, in the Fortaleza/Inconfidentes (left/right) links. Lower-row panels: mean duration of scintillation events per night during the same period, in the Fortaleza/Inconfidentes (left/right) links. The results consider nights with and without scintillation events.

It is observed that the mean numbers and durations of scintillation events in Fortaleza are consistently larger than the corresponding ones in Inconfidentes. In particular, the parameters in the latter link are essentially equal to zero after September 2016. Using the most recent version of the International Geomagnetic Reference Field model (IGRF-13) (Alken et al., 2021), the apex altitudes of field-aligned EPBs (directly above the geomagnetic equator) that intersect the IPPs (at the altitude 350 km) of the Fortaleza and Inconfidentes links have been estimated: 500 and 1,100 km, respectively. Since, particularly during the fading phase of the solar cycle, EPBs will more easily reach lower apex altitudes, it is also easier to observe EPB effects in the former than in the latter link. This argument provides a plausible explanation for the observations in the beginning of this paragraph.

The influence of the decreasing solar activity on both parameters, particularly after July 2015, is also evident in the results displayed in Figure 2. This observation is consistent with similar ones available in the earlier literature (Abdu et al., 1998; Akala et al., 2011), indicating that variations in ESF occurrence rate and intensity followed that of solar flux.

A partial list of the relevant literature indicates that the longitudinal variability of EPBs has been characterized from the analysis of in-situ data recorded by instruments onboard different satellites: AE-E (Kil & Heelis, 1998), DMSP and ROCSAT-1 (Burke et al., 2004a, 2004b; Gentile et al., 2006), C/NOFS (Huang et al., 2014), as well as by the Swarm constellation (Aa et al., 2020). In particular, the last authors have clearly demonstrated that the EPB occurrence rate is dependent on longitude, particularly in the Atlantic sector. However, Table 1 indicates that the IPP longitudes of the Fortaleza and Inconfidentes links are 35.14°W and 43.85°W ($\Delta_{lon} = 8.71$ °) and Figure 3 in the paper by Aa et al. (2020) indicates that the differences in the corresponding EPB occurrence rates of these two particular longitudes, for all seasons, are relatively small. Thus, one could expect that the contribution of the longitudinal variability contribution to the differences between the observed behaviors in Figure 2 also be relatively small.

3.2. Maximum S_4 , Duration, and Spacing Between Structures, Considering the Number of Scintillation Events per Night

Figure 3 displays the percentage of scintillation events per night for the years 2014, 2015, and 2016. These results only considered nights with at least 1 scintillation event. Their numbers and corresponding minutes are provided

MORAES ET AL. 6 of 17

15427390, 2024, 1, Downloaded from https://agupubs.onlinelibrary.wiley.com/doi/10.1029/2023SW003656, Wiley Online Library on [07/07/2024]. See the Terms and Conditions (https://agupubs.onlinelibrary.wiley.com/doi/10.1029/2023SW003656, Wiley Online Library on [07/07/2024]. See the Terms and Conditions (https://agupubs.onlinelibrary.wiley.com/doi/10.1029/2023SW003656, Wiley Online Library on [07/07/2024]. See the Terms and Conditions (https://agupubs.onlinelibrary.wiley.com/doi/10.1029/2023SW003656, Wiley Online Library on [07/07/2024]. See the Terms and Conditions (https://agupubs.onlinelibrary.wiley.com/doi/10.1029/2023SW003656, Wiley Online Library on [07/07/2024]. See the Terms and Conditions (https://agupubs.onlinelibrary.wiley.com/doi/10.1029/2023SW003656, Wiley Online Library.wiley.com/doi/10.1029/2023SW003656, Wiley Online Library.

for rules of use; OA articles are governed by the applicable Creative Commons License

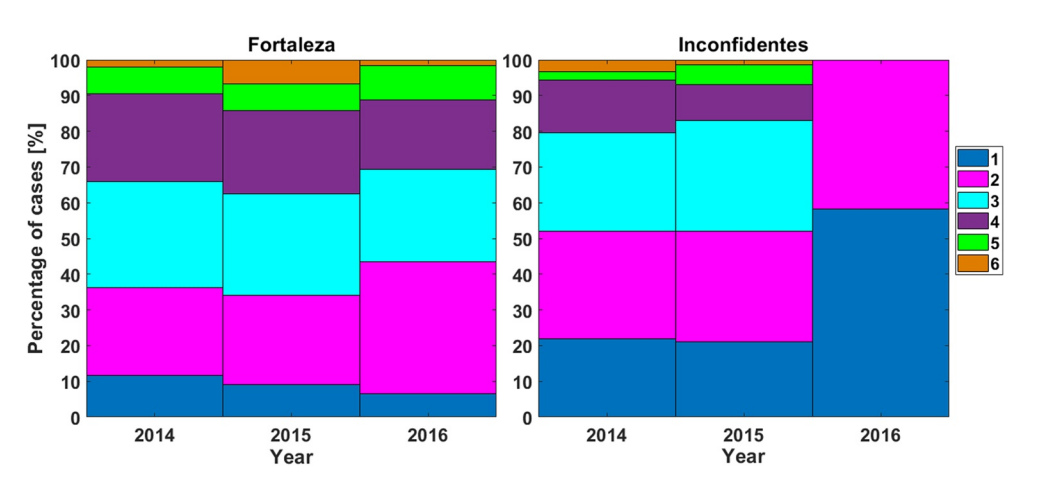


Figure 3. Percentages of the numbers of scintillation events per night in the Fortaleza/Inconfidentes links (left/right panels), during the years 2014, 2015, and 2016.

in columns 4 and 5 of Table 2. It should be stressed that this data set is also the basis for all studies to be discussed in the following sections. In rounded percentages, two or three scintillation events were observed in 60% of the nights in Fortaleza (left panel), while four scintillation events occurred in 20% of the nights. The remaining 20% were equally shared by nights with either one or five (or more) scintillation events. These percentages remained approximately the same for the 3 years. In Inconfidentes (right panel), during the years 2014 and 2015, two or three scintillation events were observed during approximately 60% of the nights - these numbers are considerably similar to those for Fortaleza. On the other hand, only one scintillation event was observed in 20% of nights and four scintillation events were observed in 10% of the nights, approximately. The occurrence of five or more scintillation event per night was relatively infrequent. Another distinct aspect is that, for the year 2016, only one and two scintillation events were observed in 60% and 40% of the nights, respectively. The 2016 results can only be explained by a decrease in the number of EPBs intersecting the Inconfidentes link as solar activity approaches its minimum, which is consistent with the discussion in the last paragraphs of Section 3.1. Therefore, the number of scintillation events observed in a single night, especially in Inconfidentes, seems to be directly connected to solar activity.

Figure 4 presents the mean values of: maximum S_4 (upper-row panels), duration of scintillation events (middle-row panels), and spacing between consecutive scintillation events (lower-row panels), both in minutes, for the Fortaleza/Inconfidentes (left/right panels) links and the 3 years, considering the position of each scintillation event in the individual night. This position is represented by a colored bar, according to the legend in the middle right-hand side of Figure 4. For example: (a) the dark blue bar in the upper-left panel and the year 2014 indicates that the mean of all maximum S_4 values for the first occurrences of scintillation events in the selected nights (whether only one or more such events occurred) is $E[\max S_4] = 0.51$; (b) the magenta bar in the middle-left panel and the same year indicates that the mean of all durations of the second occurrences of scintillation events in the selected nights (whether only two or more such events occurred) is E[duration] = 44 min.

The left panel in the upper row of Figure 4 shows that the first scintillation event had the highest $E[\max S_4]$ value in Fortaleza. The subsequent values of this parameter exhibit an essentially linear decreasing trend with the order of the scintillation event. There are no significant variations in this pattern (in absolute values or inclinations) during the analyzed years. The $E[\max S_4]$ values for the scintillation events observed in Inconfidentes are generally higher than the corresponding ones in the Fortaleza, for all years. Additionally, each value of this parameter is generally smaller than the corresponding one for the earlier year, indicating a clear influence of the decreasing solar activity. Another aspect to note is the subsequent events in the same year, for example in Inconfidentes, $E[\max(S_4)] = 0.87$ for the first scintillation events in 2014. After decreasing to 0.60 for the second scintillation events in 2014, this parameter exhibits a linear decreasing trend with the order of the scintillation event. This trend displays a faster rate than the ones in Fortaleza, but is not as regular as those patterns. On the other hand, the dependence of $E[\max(S_4)]$ on the order of the scintillation event in Inconfidentes and 2015 display the essentially linear and regular decreasing trend also observed in Fortaleza, although at a faster rate.

MORAES ET AL. 7 of 17

15427390, 2024, 1, Downloaded from https://agupubs.onlinelibrary.wiley.com/doi/10.1029/2023SW003656, Wiley Online Library on [07/07/2024]. See the Terms and Conditions (https://onlinelibrary.wiley.com.

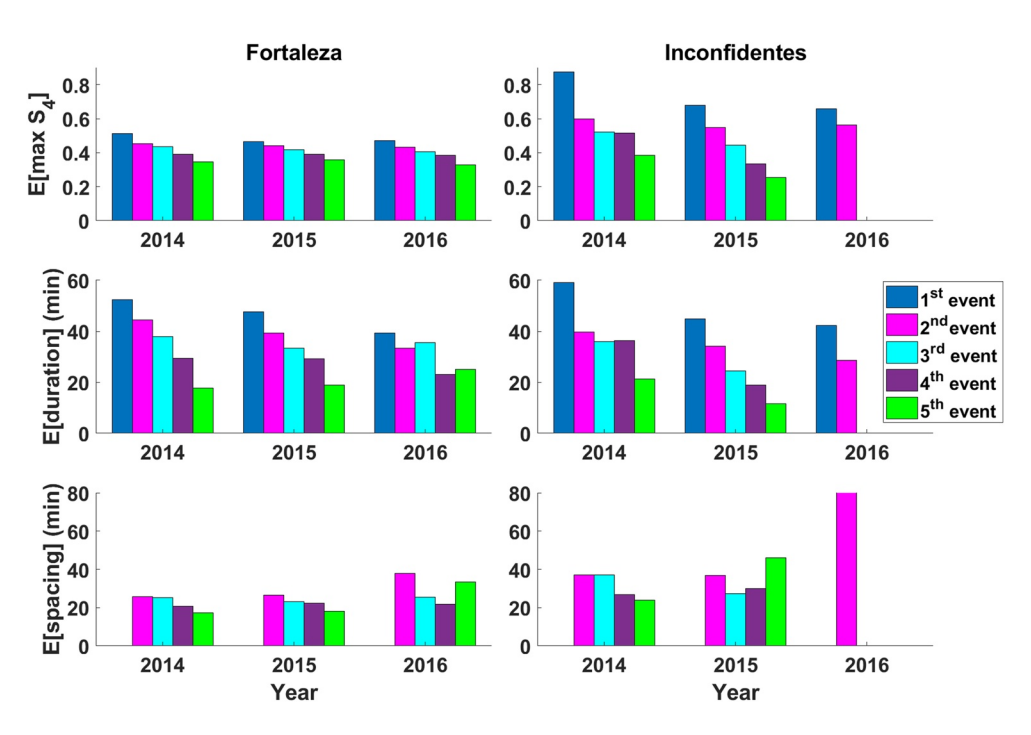


Figure 4. Mean values of maximum S_4 (upper-row panels), durations of scintillation events (middle-row panels), and spacings between consecutive scintillation events (lower-row panels) for Fortaleza/Inconfidentes (left/right panels). Each position of a scintillation event in the night is represented by a colored bar, according to the middle-right legend. The horizontal axis corresponds to the years from 2014 to 2016 (peak to near minimum of solar cycle 24, respectively).

In both links, the decrease in scintillation severity for consecutive structures may be related to the fact that the background plasma density decreases as the hours progress along the night. This change is less steep close to the equator, but more pronounced around the EIA, where the supply of plasma density due to the Equatorial Fountain Effect vanishes later at night (e.g., see Figure 4 in Silva et al., 2021). This explanation is further supported by the fast decreases of $E[\max(S_4)]$ in Inconfidentes for peak and moderate solar cycle conditions (2014 and 2015).

The panels in the middle row of Figure 4 show the mean durations of scintillation events, considering their positions in the night, for the 3 years. For both locations, it is observed that the first scintillation event has a longer mean duration, which generally decreases with the order of the subsequent structures. In general, similar patterns are observed for $E[\max(S_4)]$ and duration for the same link and year. The exception to this general rule is the difference between the $E[\max(S_4)]$ and duration patterns for Fortaleza and 2016: the latter displays oscillations on top of the more common linear decreasing trend. Additionally, it is noted that the duration patterns for Fortaleza and the years 2014 and 2015 linearly decrease at approximately the same rate.

It is worth remembering that the duration of a scintillation event depends on the irregularity zonal drift, which is known to decrease from early to-late nighttime hours (Fejer et al., 1985; Muella et al., 2008, 2017; Olwendo et al., 2016; Vargas et al., 2020). That is, one would expect a sequence of EPBs with similar widths to create a series of increasingly longer scintillation event. The results suggest the opposite, indicating that the widths of the EPBs which caused the scintillation event would decrease even faster than the observed rates. This observation is also supported by the fact that both stations, in distinct dip latitudes, observed consistent decreasing trends in the duration of consecutive scintillation events.

The panels in the lower row of Figure 4 show the mean spacings between consecutive scintillation events in the same night. The left panel indicates that, for Fortaleza and the years 2014 and 2015, the values of this parameter also exhibit an essentially linear decreasing trend with the order of the spacing between consecutive scintillation events, which are less steep than the corresponding ones for $E[\max(S_4)]$ and duration. However, the fast initial decrease observed in 2016 is reversed by the relatively long spacing between the fourth and fifth scintillation events in the nights of 2016. The right panel shows that the spacings for Inconfidentes are longer than the corresponding ones for Fortaleza. For Inconfidentes, the predominant decreasing pattern is slightly modified by the equality between the first two spacings in 2014 and strongly altered by the increase in the last two spacings in 2015. For both links, the

MORAES ET AL. 8 of 17

15427390, 2024, 1, Downloaded from https://agupubs.onlinelibrary.wiley.com/doi/10.1029/2023SW003656, Wiley Online Library on [07/07/2024]. See the Terms and Conditions (https:

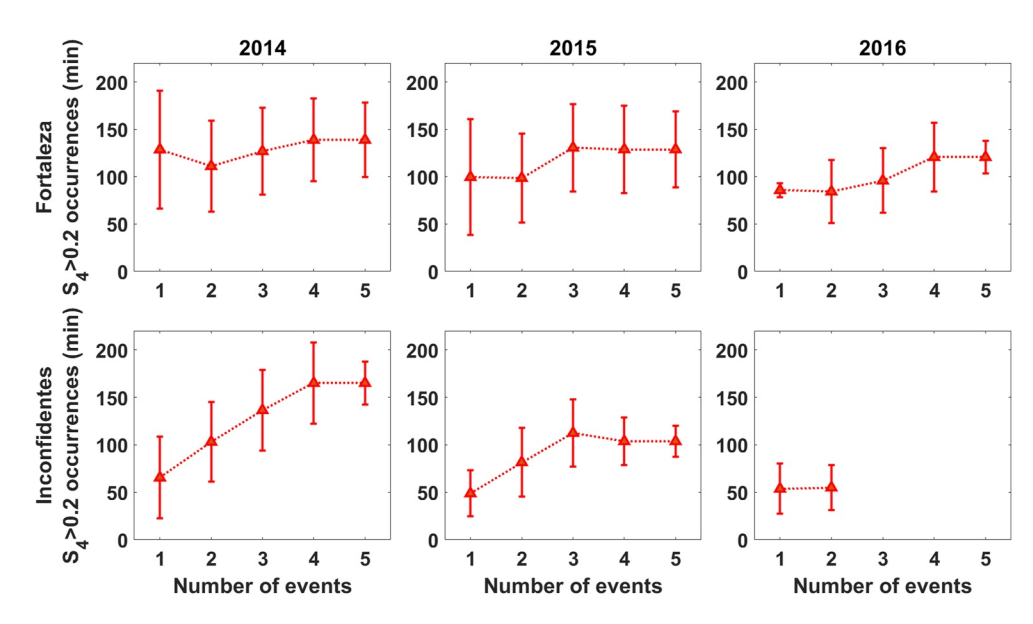


Figure 5. Mean values (central red triangles) and standard deviations (half of the vertical bars) of the total scintillation minutes ($S_4 > 0.2$) as functions of the number of scintillation events per night in Fortaleza/Inconfidentes (upper/lower panels) for the years 2014 (left panels), 2015 (middle panels), and 2016 (right panels).

interesting aspect is that, in general, the spacings are considerably smaller than the durations of the involved scintillation events. The exceptions to this observation are indicated by: (a) the green bar in the plot (Fortaleza, 2016); (b) the purple and green bars in the plot (Inconfidentes, 2015); and (c) the magenta bar in the plot (Inconfidentes, 2016).

To summarize the discussion on Figure 4, the normalized decreasing rates of the three parameters with the position of scintillation event in the night will be estimated. For each station and year, the difference between the parameter values associated with the latest and earliest event was divided by the average parameter value. It should be noted that the resulting normalized decreasing rates are dimensionless, allowing the comparison between those from different parameters. The normalized decreasing rates for Fortaleza and consecutive years and parameters are: (a) $E[\max S_4]$ (-0.38, -0.26, -0.36); (b) E[duration] (-0.96, -0.85, -0.45); and (c) E[spacing] (-0.38, -0.37, NA). Those for Inconfidentes are: (d) $E[\max S_4]$ (-0.43, -0.94, -0.16); (e) E[duration] (-0.99, -1.24, -0.39); and (f) E[spacing] (-0.42, NA, NA). The acronym NA (not available) indicates which normalized decreasing rate values were not calculated (the ones associated with E[spacing] for Fortaleza and the year 2016; and for Inconfidentes and the years 2015 and 2016). It is noted that the Inconfidentes $E[\max(S_4)]$ pattern for 2015 and the Fortaleza/Inconfidentes duration patterns for 2014 and 2015 linearly decrease at approximately the same normalized rate, which is faster than all the other available ones.

The next analysis investigated how the number of scintillation events relate to the total scintillation time, per night. For each night, the number of scintillation events was related to the sum of their durations (both determined according to the procedures in Section 2).

The upper/lower panels of Figure 5 display the mean value (represented by a central red triangle) and standard deviation (half of the vertical bar) of the total number of scintillation minutes (with $S_4 > 0.2$) per night for Fortaleza/Inconfidentes in 2014 (left panels), 2015 (middle panels), and 2016 (right panels), based on different numbers of scintillation events. These results, in principle, differ from those presented in the middle row of Figure 4, which focus on the durations of scintillation events. Specifically, the current results determine the mean number of minutes with $S_4 > 0.2$ associated with occurrences of a single scintillation event per night, two scintillation events per night, and so on. In contrast, the previous results estimate the mean durations of the first scintillation event of the night, the second scintillation event of the night, regardless of the number of occurrences, and so forth.

The Fortaleza results for 2014 indicate that the mean value of the total number of scintillation minutes per night remained essentially unchanged (varying between 111 and 139 min), regardless of the number of scintillation events per night. For 2015, the parameter increased from 100 to 131 min when the number of scintillation events

MORAES ET AL. 9 of 17

15427390, 2024, 1, Downloaded from https://agupubs.onlinelibrary.wiley.com/doi/10.1029/2023SW003656, Wiley Online Library on [07/07/2024]. See the Terms and Conditions (https://agupubs.onlinelibrary.wiley.com/doi/10.1029/2023SW003656, Wiley Online Library on [07/07/2024]. See the Terms and Conditions (https://agupubs.onlinelibrary.wiley.com/doi/10.1029/2023SW003656, Wiley Online Library on [07/07/2024]. See the Terms and Conditions (https://agupubs.onlinelibrary.wiley.com/doi/10.1029/2023SW003656, Wiley Online Library on [07/07/2024]. See the Terms and Conditions (https://agupubs.onlinelibrary.wiley.com/doi/10.1029/2023SW003656, Wiley Online Library on [07/07/2024]. See the Terms and Conditions (https://agupubs.com/doi/10.1029/2023SW003656, Wiley Online Library.wiley.com/doi/10.1029/2023SW003656, Wiley Online Library.

ns) on Wiley Online Library for rules of use; OA articles are governed by the applicable Creative Commons License

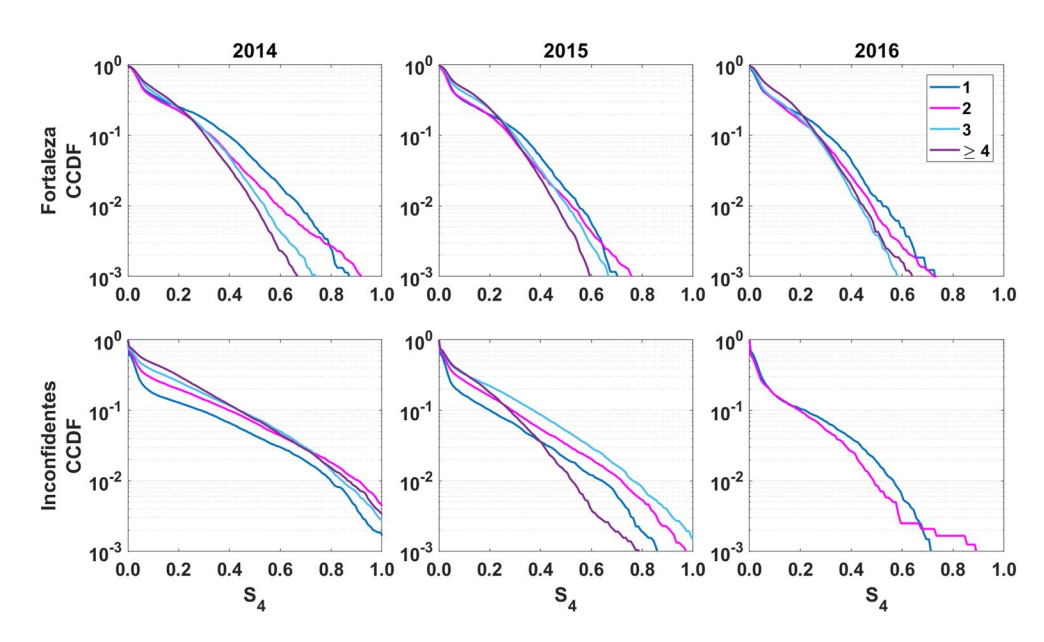


Figure 6. Complementary cumulative distribution functions of S_4 in the Fortaleza/Inconfidentes links (upper/lower panels), for 2014 (left panels), 2015 (middle panels), and 2016 (right panels), considering different numbers of scintillation events per night, represented by the color scheme in the upper-right legend.

varied from two or less to three or more per night. For 2016, the parameter increased from 84 to 121 min when the number of scintillation events varied from two or less to four or more per night. The standard deviation of the total scintillation minutes per night remained mostly around 50 min throughout the years.

The dependence of the mean value of the total number of scintillation minutes on the number of scintillation events per night in Inconfidentes (lower panels) exhibits considerably distinct patterns. For 2014, the parameter linearly increased from 65 to 162 min when the number of scintillation events varied from one to four per night, remaining at the latter value for five events. For 2015, the parameter linearly increased from 50 to 110 min when the number of scintillation events varied from one to three per night. Then, it slightly decreased to 100 min for four and five scintillation events per night. For 2016, the parameter remained constant at 55 min for one and two scintillation events per night. It is worth remembering that, for the Inconfidentes link: (a) nights with more than four scintillation events were relatively rare in 2015; and (b) only nights with one or two scintillation events were observed in 2016, as shown in Figure 3. The standard deviation of the total scintillation minutes per night remained essentially constant, at approximately 43 min, 36 min, and 26 min, for the years 2014, 2015, and 2016, respectively.

In summary, the mean value of the total number of scintillation minutes in Fortaleza remained roughly independent from the number of scintillation events per night, slightly decreasing through the 3 years. The standard deviation of the total scintillation minutes per night remained essentially constant in the same time frame. The same behavior is observed in Inconfidentes during 2016. However, the mean value of the total number of scintillation minutes in Inconfidentes initially increased with the number of scintillation events per night in 2014 and 2015, before reaching a relatively constant value. The standard deviation of the total scintillation minutes per night remained essentially constant in the same time frame. In Inconfidentes, the values of corresponding parameters also generally decreased along the years. For one scintillation event per night, the mean values of the total number of scintillation minutes in Fortaleza are approximately twice the corresponding ones for Inconfidentes, regardless of the year.

After contributing to a better understanding of the average number of scintillation events per night, as well as their durations and spacings, it is important to identify scenarios that are less favorable to GNSS users. To do so, Figure 6 displays complementary cumulative distribution functions (CCDFs) of S_4 in a similar way to that adopted by Salles et al. (2021). That is, CCDF(S_4) = N_{S_4}/N , where: (a) N_{S_4} is the number of occurrences of amplitude scintillation indices above each of the selected S_4 values in all nights of the year and station that display the particular number of events; and (b) N is the total number of minutes in all nights of the year and station that display the same number of events. Thus, the CCDFs in Figure 6 are parameterized by the number of scintillation

MORAES ET AL. 10 of 17

10.1029/2023SW003656

Space Weather

events detected per night in the Fortaleza/Inconfidentes links (upper/lower panels), during the years 2014 (left panels), 2015 (middle panels), and 2016 (right panels), according to the color code indicated by the legend inside the upper-right panel.

As previously observed in the upper row of Figure 5, the increase in the number of scintillation events in the Fortaleza link did not necessarily lead to an increase in the number of scintillation minutes per night. This is confirmed by the panels in the upper row of Figure 6, which shows that $Pr\{S_4 > 0.2\}$ is essentially independent from the former parameter. On the other hand, the same panels show that $Pr\{S_4 > 0.2\}$ depends on the number of scintillation events per night. For each of the 3 years, these probabilities, for one or two scintillation events (which tend to have longer durations, according to the middle-row panels in Figure 4), are greater than those for three or more events.

The panels in the lower row of Figure 6 show that, in the Inconfidentes link, $Pr\{S_4 > 0.2\}$ and $Pr\{S_4 > 0.7\}$ for one scintillation event per night are generally smaller than those for two or more events, in agreement with the results in the lower row of Figure 5. The exceptions are: (a) $Pr_1\{S_4 > 0.7\} > Pr_4\{S_4 > 0.7\}$, where the first indices indicate the number of scintillation events per night; and (b) the results for 2016.

It is also observed that, particularly when $S_4 > 0.6$, the Inconfidentes probabilities are greater than the corresponding ones for Fortaleza, consistently with the locations of the two sites (close to the southern crest of the EIA and to the equatorial region, respectively). Again, the influence of the solar cycle is noted in the results from the two links, with the 2014 CCDFs showing higher values when compared to those for the other years, confirming the findings by Moraes, Muella, et al. (2018).

It should be stressed that the probabilities in Figure 6 are conditioned to the occurrences of one or more scintillation events per night. Indeed, the conditional probabilities $Pr\{S_4 > 0.7\}$ at least 1 event} resulting from the ratios between the corresponding values in columns 8 and five of Table 2 for Fortaleza, Inconfidentes, and the 3 years are $(2.97 \times 10^{-3}, 8.83 \times 10^{-4}, 7.15 \times 10^{-4})$ and $(2.79 \times 10^{-2}, 1.10 \times 10^{-2}, 2.00 \times 10^{-2})$, respectively. These probabilities are consistent with the corresponding mean ones observed in Figure 6. However, the absolute probabilities $Pr\{S_4 > 0.7\}$ resulting from the ratios between the corresponding values in columns 8 and 3 of Table 2, which also consider nights without scintillation events, are relatively smaller and may provide a more faithful representation of the impact of scintillation upon GNSS users: $(1.54 \times 10^{-3}, 4.12 \times 10^{-4}, 1.81 \times 10^{-4})$ and $(1.04 \times 10^{-2}, 2.30 \times 10^{-3}, 7.77 \times 10^{-4})$. Costa et al. (2020) used time series of the standard deviation of the ion density fluctuations δNi obtained in situ by the C/NOFS PLP. The values of this parameter were corrected for its average dependence on the geomagnetic latitude and the result mapped into S_4 , using a modified version of a well-known single-scattering model (Rino, 1979, 2011). The resulting CCDF for the South-American sector estimated $Pr\{S_4 > 0.7\} \approx 1.00 \times 10^{-3}$, which is in reasonable agreement with the absolute probability for Fortaleza during 2014, considering the differences in the solar activities in the two years (Costa et al., 2020).

3.3. Characteristics of Scintillation Events Along the Night

The previous discussions focused on scintillation event characteristics, according to season and activity of the solar cycle. In this section, the temporal changes in scintillation event characteristics along the night will be addressed.

The first characteristic to be analyzed is how the maximum S_4 in a scintillation event changes along the night, considering their occurrence orders. Beginning at 18:00 LT, for each one-hour interval containing the start of a scintillation event, the maximum S_4 and the event order were annotated. Then, for each one-hour interval and event order, the mean value and standard deviation of the corresponding collection of maximum S_4 values were estimated. These values were assigned to the center of the one-hour interval and to the event order. The upper/lower panels of Figure 7 show the results for the Fortaleza/Inconfidentes links, during 2014 (left), 2015 (middle), and 2016 (right), using the same convention of Figure 5. The orders of scintillation events in the night are represented by different colors, according to the legend displayed at the lower-right panel.

The $E[\max S_4]$ values for Fortaleza are relatively small, typically less than 0.5. While the corresponding values for the first scintillation event in 2014 and 2015 display an increasing trend along the night hours, the others slightly decrease or remain essentially constant. The observed characteristic does not considerably change over the years, in agreement with the results presented in the upper-left panel of Figure 4.

MORAES ET AL. 11 of 17

15427390, 2024, 1, Downloaded from https://agupubs.onlinelibrary.wiley.com/doi/10.1029/2023SW003656, Wiley Online Library on [07/07/2024]. See the Terms and Conditions (https://agupubs.onlinelibrary.wiley.com/doi/10.1029/2023SW003656, Wiley Online Library on [07/07/2024]. See the Terms and Conditions (https://agupubs.com/doi/10.1029/2023SW003656, Wiley Online Library on [07/07/2024]. See the Terms and Conditions (https://agupubs.com/doi/10.1029/2023SW003656, Wiley Online Library on [07/07/2024]. See the Terms and Conditions (https://agupubs.com/doi/10.1029/2023SW003656, Wiley Online Library on [07/07/2024]. See the Terms and Conditions (https://agupubs.com/doi/10.1029/2023SW003656, Wiley Online Library on [07/07/2024]. See the Terms and Conditions (https://agupubs.com/doi/10.1029/2023SW003656, Wiley Online Library on [07/07/2024]. See the Terms and Conditions (https://agupubs.com/doi/10.1029/2023SW003656, Wiley Online Library on [07/07/2024]. See the Terms and Conditions (https://agupubs.com/doi/10.1029/2023SW003656, Wiley Online Library on [07/07/2024]. See the Terms and Conditions (https://agupubs.com/doi/10.1029/2023SW003656, Wiley Online Library on [07/07/2024]. See the Terms and Conditions (https://agupubs.com/doi/10.1029/2023SW003656, Wiley Online Library on [07/07/2024]. See the Terms and Conditions (https://agupubs.com/doi/10.1029/2023SW003656, Wiley Online Library on [07/07/2024]. See the Terms and Conditions (https://agupubs.com/doi/10.1029/2023SW003656, Wiley Online Library on [07/07/2024]. See the Terms and Conditions (https://agupubs.com/doi/10.1029/2023SW003656, Wiley Online Library on [07/07/2024]. See the Terms and Conditions (https://agupubs.com/doi/10.1029/2023SW003656, Wiley Online Library on [07/07/2024]. See the Terms and Conditions (https://agupubs.com/doi/10.1029/2023SW003656, Wiley Online Library on [07/07/2024]. See the Terms and Conditions (https://agupubs.com/doi/10.1029/2023SW003656, Wiley Online Library on [07/07/2024]. See the Terms and Conditions (https://agupubs.com/doi/10.1029/2

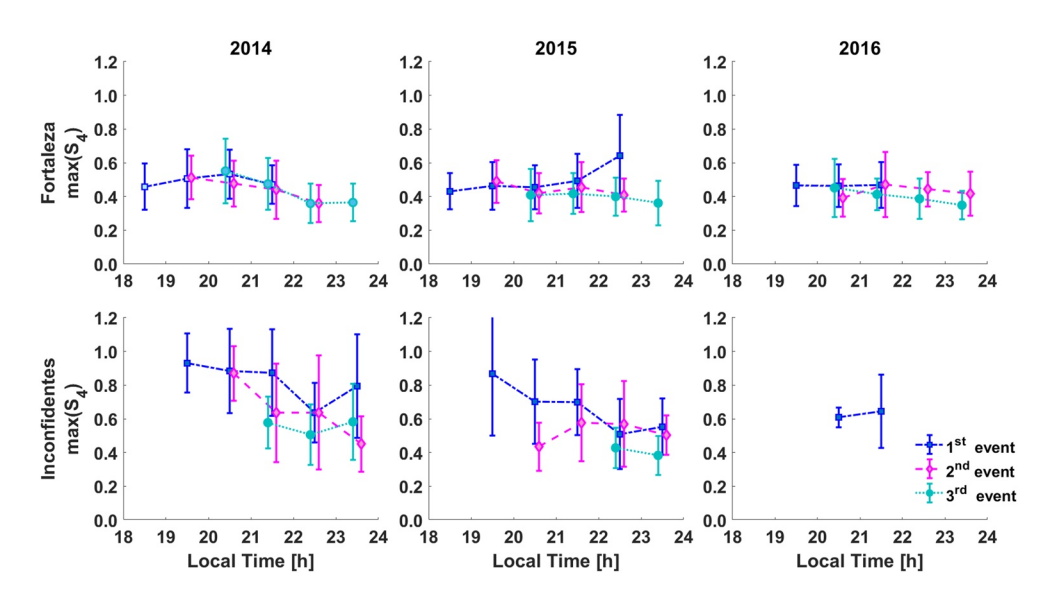


Figure 7. Mean values and standard deviations of the maximum value of S_4 along the night hours, considering the order of scintillation events, for Fortaleza/Inconfidentes (upper/lower panels), during the years 2014 (left panels), 2015 (middle panels), and 2016 (right panels). Each scintillation event is identified by a proper color, according to the legend in the lower-right panel.

In Inconfidentes and the first 2 years, the $E[\max S_4]$ values for the first scintillation event start with large values (close to 0.9) and decay more steeply along the night. This observation is also valid for the second scintillation event in 2014. On average, the $E[\max S_4]$ values seem to decrease for consecutive scintillation events and as the solar activity decays (from left to right panels), again in conformity with the upper right panel of Figure 4. The relative values of $E[\max S_4]$ in the upper and lower panels of Figure 7 are consistent with the locations of the associated IPPs, close to the geomagnetic equator and to the southern crest of EIA, respectively.

Naturally, low-order scintillation events started earlier than late-order ones. In both sites, scintillation events started later in 2016 than the corresponding ones in 2014 and 2015. Additionally, scintillation events started earlier in Fortaleza than the corresponding ones in Inconfidentes. This observation was expected from an EPB time evolution after its generation at the geomagnetic equator, which combines an upward motion with an increase in latitudinal extent, keeping the geomagnetic-field alignment. Therefore, IPPs that are close to the geomagnetic equator will be intersected by EPBs earlier than those located under the southern crest of EIA.

The same procedures were then applied to the evolutions of scintillation event durations along the night hours, considering their occurrence orders. Figure 8 shows the mean values and standard deviations of this parameter for Fortaleza/Inconfidentes (upper/lower panels) and the years 2014 (left), 2015 (middle), and 2016 (right). In both stations, local time seems to be a relevant factor: scintillation events are longer in the early nighttime, shortening along the night. It should be remembered that the typical EPB zonal drift pattern also decreases along the nighttime hours. Therefore, the decrease in EPB widths along the hours may be even steeper that those observed in Figure 8. It is also noted that the average durations of consecutive scintillation events at most local times have similar values for both stations, indicating that the underlying mechanisms related to event and EPB dimensions may be more related to local time than previously believed.

In Fortaleza and the first 2 years, the first scintillation event can occur as early as during the initial time interval (from 18:00 LT to 19:00 LT), but later onsets are also observed (from 19:00 LT to 23:00 LT). In the same link and years, the second scintillation event is usually detected between 19:00 LT and 23:00 LT, while the onset of the third one may extend to midnight. In the same link and 2016, most onsets occurred 1 hr later than the corresponding ones in the previous years. Similar trend in the spatiotemporal development of scintillation over the Brazilian region was recently discussed by Sousasantos et al. (2024).

For all event orders in Inconfidentes, during the first 2 years: (a) most first onsets are observed 1 hour later than the corresponding ones in Fortaleza; and (b) the onsets can occur until midnight. This observation is consistent with the times reported by Sousasantos et al. (2018) and can be attributed to the greater geomagnetic latitude of Inconfidentes

MORAES ET AL. 12 of 17

15427999, 2024. 1, Downloaded from https://agupubs.onlinelibrary.wiley.com/doi/10.1029/2023SW003656, Wiley Online Library on [07/07/2024]. See the Terms and Conditions (https://onlinelibrary.wiley.com/terms-and-conditions) on Wiley Online Library for rules of use; OA articles are governed by the applicable Creative Commons License

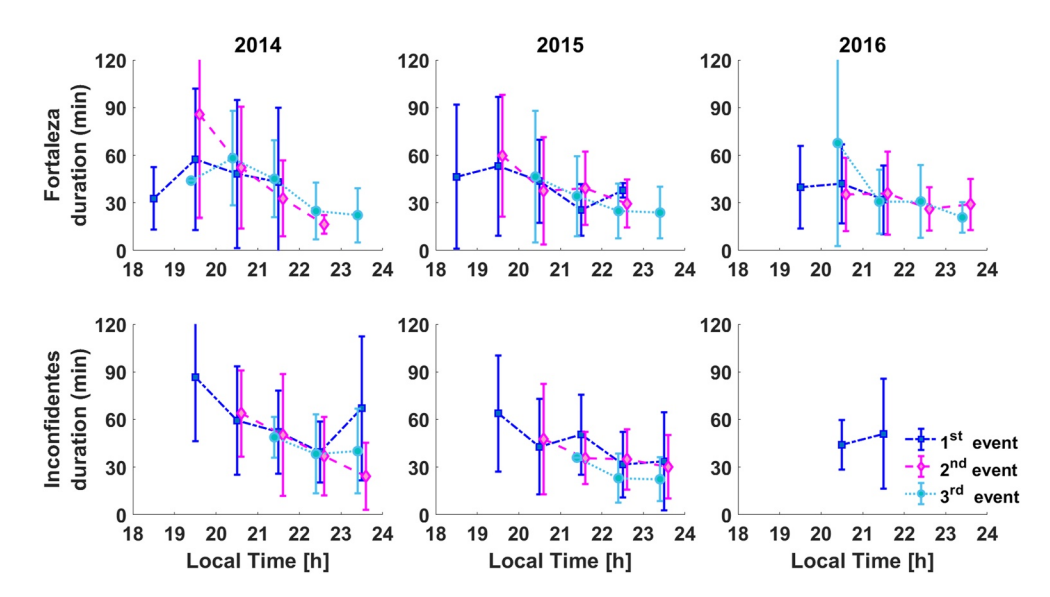


Figure 8. Mean values and standard deviations of scintillation event durations along the night hours, considering the event order, for Fortaleza/Inconfidentes (upper/lower panels), during the years of 2014 (left panels), 2015 (middle panels), and 2016 (right panels). Each scintillation event is identified by a proper color, according to the legend in the lower-right panel.

when compared to that of Fortaleza, as explained above. In 2016, the first scintillation event in Inconfidentes appeared between 20:00 LT and 21:00 LT, which is later than in other years, and only extended for another hour.

The very few cases occurring after midnight and for greater occurrence orders in Inconfidentes during 2016 were not included in the analysis, due to their lack of statistical significance.

The dependence of spacings between consecutive scintillation events on night hours, considering their occurrence orders, was the next analyzed characteristic, using the procedures already described. Figure 9 shows the mean values and standard deviations of this parameter for Fortaleza/Inconfidentes (upper/lower panels) and the years 2014 (left panels), 2015 (middle panels), and 2016 (right panel, only for Fortaleza). The results from both sites indicate that the mean spacing increases as the night progresses, regardless of the event order. They

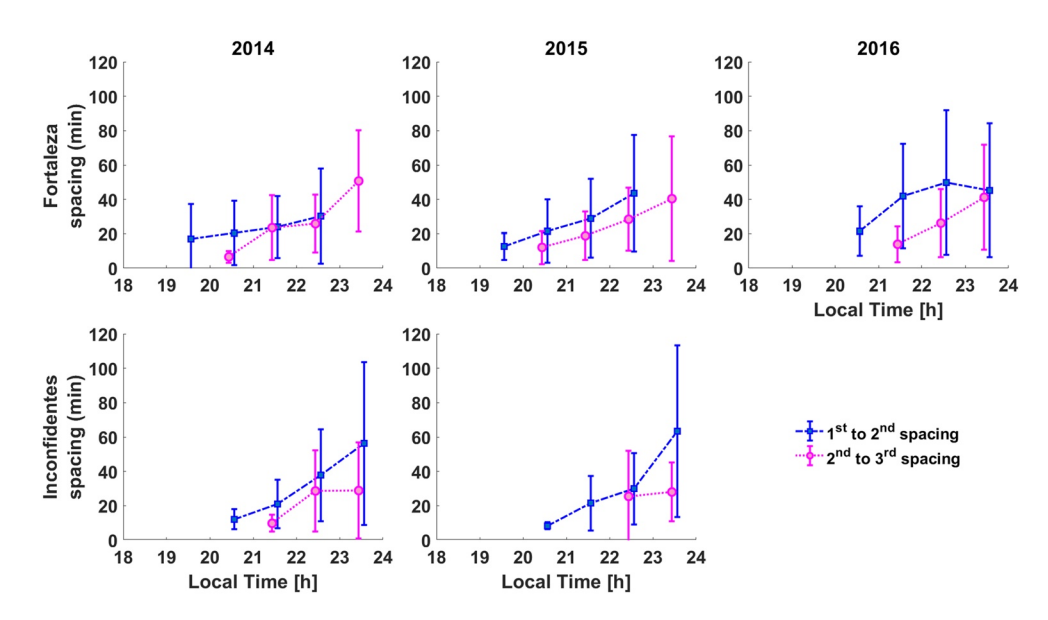


Figure 9. Mean values and standard deviations of spacings between consecutive scintillation events along the night hours, considering the event orders, for Fortaleza/Inconfidentes (upper/lower panels), during the years of 2014 (left panels), 2015 (middle panels), and 2016 (right panel, only for Fortaleza). Each scintillation event is identified by a proper color, according to the legend in the lower-right panel.

MORAES ET AL. 13 of 17

15427390, 2024, 1, Downloaded from https://agupubs.onlinelibrary.wiley.com/doi/10.1029/2023SW003656, Wiley Online Library on [07/07/2024]. See the Terms and Condition

of use; OA articles are governed by the applicable Creative Commons License

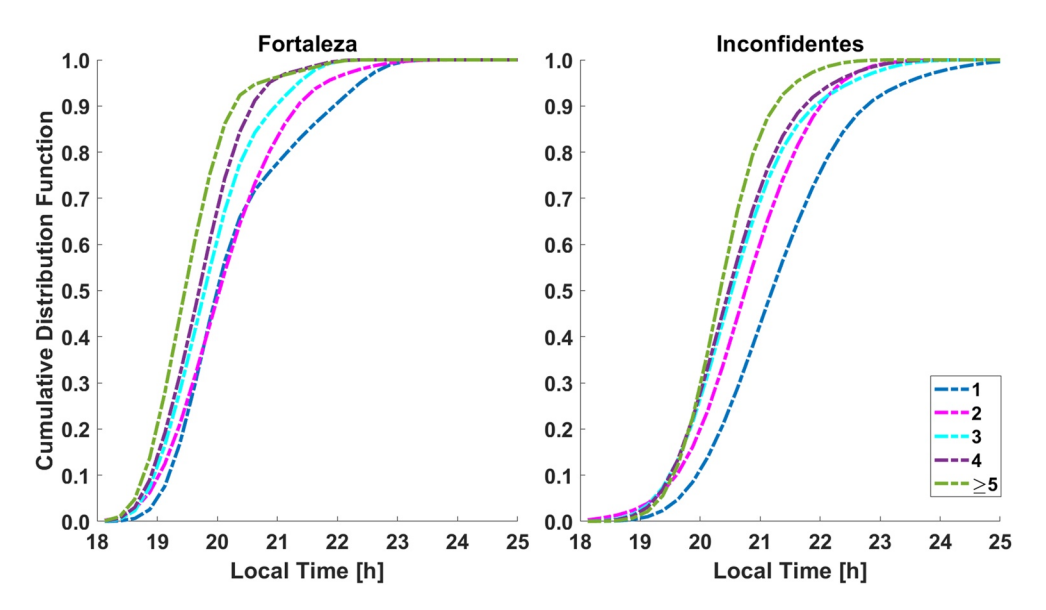


Figure 10. Cumulative distribution functions (CDFs) of the scintillation onset time (that of the first occurrence of $S_4 > 0.2$ in the night), considering different number of scintillation events per night for Fortaleza/Inconfidentes (left/right panels). Each CDF is identified by a proper color, according to the legend in the right panel.

also show that, for the same time window and each site, the spacings between the second and third scintillation events are generally shorter than the corresponding ones between the first and second events. Additionally, for the same time window and each event order, the Fortaleza spacings are generally greater than the corresponding ones in Inconfidentes. The standard deviation bars show increasing patterns, regardless of the station and year, indicating the large day-to-day variability of the scintillation events. Again, EPB drift velocities are expected to decrease along the night (Fejer et al., 1985; Muella et al., 2008, 2017; Olwendo et al., 2016; Vargas et al., 2020). This would also explain, at least in part, the longer spacings between events later in the evening.

Figure 10 shows the results from the final analysis: the empirical cumulative distribution functions (CDFs) of the scintillation onset time (that of the first occurrence of $S_4 > 0.2$ in the night) for Fortaleza/Inconfidentes (left/right panels) during the 3 years, considering the number of events per night (ranging from one to five or more, according to the legend in the right panel). A similar behavior is observed in the CDFs of both stations: the probability of an early onset increases with the number of scintillation event per night. For example, for one and five or more scintillation events per night, the probabilities of scintillation onsets: (a) before 19:00 LT in Fortaleza are equal to 0.05 and 0.20; and (b) before 20:30 LT in Inconfidentes are equal to 0.27 and 0.63; respectively. In addition, as expected with basis on previous explanation, the Inconfidentes onset times, for the same probability level and number of events per night, occurs one to 2 hr later than the corresponding ones in Fortaleza. This information is valuable, because the onset time can serve as an indicator of the probable number of scintillation events for the night. That is, the later the onset time, the fewer scintillation events should be expected, and vice-versa, as quantified in Figure 10. These results, along with those in Figures 5 and 6, suggest that the early scintillation onset time in Inconfidentes is related to more probable longer and severe S_4 cases, due to the greater number of scintillation events in that night. Conversely, the occurrence of a single scintillation event suggests the same less favorable scenario in Fortaleza.

4. Conclusion

In this work, data recorded by two stations in distinct dip latitudes were used to evaluate several characteristics of scintillation events occurring within the time interval from 18:00 LT to 02:00 LT during the years 2014–2016. The IPPs of the Fortaleza and Inconfidentes links from geostationary SBAS satellites are close to the equator and the southern crest of the EIA, respectively. The links had elevation angles greater than 40° . The occurrences of scintillation events were identified with basis on the S_4 index. The evaluated characteristics of these events were

MORAES ET AL. 14 of 17

Space Weather

10.1029/2023SW003656

the maximum S_4 within each structure, their durations, and spacings between consecutive ones, if available. The main findings of this work were:

- The seasonal analysis is consistent with previous studies in the literature: in both links, scintillation occurs from September to March (Stolle et al., 2008; and references therein). In both links, for the number of scintillation events and their durations per night: (a) the values associated with October or November tended to be larger than those associated with September and December; (b) for the clusters centered on January 2015 and January 2016, the values associated with February tended to be larger than those associated with January and March; and (c) the values associated with January 2014 or March 2014 generally exceeded those associated with February 2014.
- In Fortaleza, during the 3 years and considering the defined thresholds, the most likely numbers of observed scintillation events per night were two or three. This also holds during the first 2 years in Inconfidentes. However, in 2016, as the solar activity fades, Inconfidentes (more distant from the geomagnetic equator) mostly observed the occurrence of only 1 scintillation event per night.
- On average, the first scintillation event usually had larger maximum S₄ values when compared to those of the
 later ones along the night. Moreover, the first scintillation event had a longer mean duration than the succeeding ones in a given night. Due to these characteristics, the first scintillation event in a given night may be
 considered as the most deleterious one to transionospheric L1 signals.
- The total of scintillation minutes (with $S_4 > 0.2$) in Fortaleza oscillated by up to 30% around approximately 120 min, regardless of the number of scintillation events observed per night and year. In Inconfidentes, the trend is distinct: the total of scintillation minutes per night linearly increased with the number of observed scintillation events, but decreased as solar activity reduces.
- The Fortaleza S₄ CCDFs (conditioned to the number of events per night) indicated higher probabilities of intense scintillation (Pr{S₄ > 0.7}) for the occurrence of a single scintillation event per night. Users under such conditions are likely to experience intense scintillation more frequently than they would if there were multiple scintillation events in the same night. On the other hand, in Inconfidentes, an increase in the number of scintillation events per night tends to also increase the probabilities of intense scintillation. In general, the Fortaleza CCDF values are smaller than the Inconfidentes corresponding ones, particularly for 2014 and 2015. Additionally, the CCDF values for both stations tend to decrease as the solar activity fades.
- The evolution of E[max S₄] along the night hours indicated the relevance of the local time on the this parameter, particularly in Inconfidentes.
- It was found that the duration of the observed scintillation events tended to decrease with local time. The spacing between consecutive events, however, increased with local time.
- The empirical CDFs of the scintillation onset time (that of the first occurrence of S₄ > 0.2 in the night) indicated that the Inconfidentes values of this parameter, for the same probability level and number of events per night, occurred one to 2 hour later than the corresponding ones in Fortaleza, in agreement with results by Sousasantos et al. (2018). Additionally, early occurrences of onset times are related to the increased probability of the occurrence of multiple scintillation events, and vice-versa.

Based on the present results, future studies may discuss SBAS operation under scintillation in the region (in terms of bit error rates, as well as other performance and availability metrics). Additionally, it should be noted that relations between the analyzed parameters and those of EPBs have only been presented here in general and approximate terms. There are difficulties in the inference of EPB features from ground-received scintillation signals. Indeed, it should be remembered that scintillation signals received on the ground integrate and combine the effects from radio wave propagation through complex EPBs and their embedded irregularity structures, distributed over a thick ionospheric layer. For example, they can be related to separate EPBs generated through time or to bifurcated structures from a single EPB. Inferring EPB features from ground-received scintillation signals duration and spacing also depend on adopted criteria, as well as on irregularity drifts and the resulting time scale of scintillation. Future studies may analyze these relations more closely, also based on simultaneous additional in-situ or ground-based (radar or optical imaging) data. They would additionally benefit from predictions by computer simulation models which integrate the development of three-dimensional EPBs and their structures with simultaneous scintillation calculations.

MORAES ET AL. 15 of 17

15427390, 2024, 1, Downloaded from

are governed by the applicable Creative Comm

Data Availability Statement

The scintillation data used in this paper is available to download through the CIGALA/CALIBRA website: https://ismrquerytool.fct.unesp.br/is/index.php. Authors would like to thank the International Association of Geomagnetism and Aeronomy (IAGA) and all the scientific and technical staff responsible for the distribution of the International Geomagnetic Reference Field (IGRF). The authors acknowledge the NASA Space Physics Data Facility staff. The OMNI data (F10.7) were obtained from the GSFC/SPDF OMNIWeb interface at https://omniweb.gsfc.nasa.gov.

Acknowledgments

This work has been performed in the framework of the INCT GNSS-Na-vAer Project under grants CNPq 465648/2014-2 and FAPESP 2017/50115-0. AM, EC, JFGM are respectively grateful to PQ 309389/2021-6, PQ 305984/2019-5, PQ 304773/2021-2. Work at UT Dallas is supported by NSF awards AGS-1916055 and AGS-2122639.

References

- Aa, E., Zou, S., & Liu, S. (2020). Statistical analysis of equatorial plasma irregularities retrieved from Swarm 2013–2019 observations. *Journal of Geophysical Research: Space Physics*, 125(4), e2019JA027022. https://doi.org/10.1029/2019JA027022
- Abdu, M. A., Sobral, J. H. A., Batista, I. S., Rios, V. H., & Medina, C. (1998). Equatorial spread-F occurrence statistics in the American longitudes: Diurnal, seasonal and solar cycle variations. Advances in Space Research, 22(6), 851–854. https://doi.org/10.1016/S0273-1177(98)00111-2
- Akala, A. O., Doherty, P. H., Valladares, C. E., Carrano, C. S., & Sheehan, R. (2011). Statistics of GPS scintillations over South America at three levels of solar activity. *Radio Science*, 46(05), RS0D24. https://doi.org/10.1029/2011RS004678
- Alken, P., Thébault, E., Beggan, C. D., Amit, H., Aubert, J., Baerenzung, J., et al. (2021). International geomagnetic reference field: The thirteenth generation. *Earth Planets and Space*, 73(1), 1–25. https://doi.org/10.1186/s40623-020-01288-x
- Burke, W. J., Gentile, L. C., Huang, C. Y., Valladares, C. E., & Su, S.-Y. (2004). Longitudinal variability of equatorial plasma bubbles observed by DMSP and ROCSAT. *Journal of Geophysical Research*, 109(A12), A12301. https://doi.org/10.1029/2004JA010583
- Burke, W. J., Huang, C. Y., Gentile, L. C., & Bauer, L. (2004). Seasonal-longitudinal variability of equatorial bubble occurrence. *Annales Geophysicae*, 22(9), 3089–3098. https://doi.org/10.5194/angeo-22-3089-2004
- Caton, R. G., & Groves, K. M. (2006). Longitudinal correlation of equatorial ionospheric scintillation. *Radio Science*, 41(5), RS5S22. https://doi.org/10.1029/2005RS003357
- Costa, E., Roddy, P. A., & Ballenthin, J. O. (2020). Space diversity mitigation effects on ionospheric amplitude scintillation with basis on the analysis of C/NOFS planar Langmuir probe data. *Radio Science*, 55(12), e2020RS007085. https://doi.org/10.1029/2020RS007085
- Costa, E., Roddy, P. A., Ballenthin, J. O., & Groves, K. M. (2018). Statistics of durations and spacings of equatorial plasma depletions detected by the C/NOFS Planar Langmuir Probe. Space Weather, 16(7), 870–886. https://doi.org/10.1029/2018SW001901
- Dabas, R. S., & Reddy, B. M. (1990). Equatorial plasma bubble rise velocities in the Indian sector determined from multistation scintillation observations. *Radio Science*, 25(2), 125–132. https://doi.org/10.1029/RS025i002p00125
- de Paula, E. R., Monico, J. F. G., Tsuchiya, I. H., Valladares, C. E., Costa, S. M. A., Marini-Pereira, L., et al. (2023). A retrospective of global navigation satellite system ionospheric irregularities monitoring networks in Brazil. *Journal of Aerospace Technology and Management*, 15, e0123. https://doi.org/10.1590/jatm.v15.1288
- Dungey, J. W. (1956). Convective diffusion in the equatorial F region. Journal of Atmospheric and Terrestrial Physics, 9(5–6), 304–310. https://doi.org/10.1016/0021-9169(56)90148-9
- Fejer, B. G., Kudeki, E., & Farley, D. T. (1985). Equatorial F region zonal plasma drifts. Journal of Geophysical Research, 90(A12), 12249–12255. https://doi.org/10.1029/JA090iA12p12249
- Gentile, L. C., Burke, W. J., & Rich, F. J. (2006). A global climatology for equatorial plasma bubbles in the topside ionosphere. Annales Geophysicae, 24(1), 163–172. https://doi.org/10.5194/angeo-24-163-2006
- Gentile, L. C., Burke, W. J., Roddy, P. A., Retterer, J. M., & Tsunoda, R. T. (2011). Climatology of plasma density depletions observed by DMSP in the dawn sector. *Journal of Geophysical Research*, 116(A3), A03321. https://doi.org/10.1029/2010JA016176
- Huang, C.-S., de La Beaujardiere, O., Roddy, P. A., Hunton, D. E., Liu, J. Y., & Chen, S. P. (2014). Occurrence probability and amplitude of equatorial ionospheric irregularities associated with plasma bubbles during low and moderate solar activities (2008–2012). *Journal of Geophysical Research: Space Physics*, 119(A2), 1186–1199. https://doi.org/10.1002/2013JA019212
- Huba, J. D., Wu, T. W., & Makela, J. J. (2015). Electrostatic reconnection in the ionosphere. *Geophysical Research Letters*, 42(6), 1626–1631. https://doi.org/10.1002/2015GL063187
- Kelley, M. C. (1989). The Earth's ionosphere: Plasma physics and electrodynamics (Vol. 43). Academic Press.
- Keskinen, M. J., Ossakow, S. L., Basu, S., & Sultan, P. J. (1998). Magnetic-flux-tube-integrated evolution of equatorial ionospheric plasma bubbles. *Journal of Geophysical Research*, 103(A3), 3957–3967. https://doi.org/10.1029/97JA02192
- Kil, Y., & Heelis, R. A. (1998). Global distribution of density irregularities in the equatorial ionosphere. *Journal of Geophysical Research*, 103(A1), 407–417. https://doi.org/10.1029/97JA02698
- Monico, J. F. G., de Paula, E. R., Moraes, A. O., Costa, E., Shimabukuro, M. H., Alves, D. B. M., et al. (2022). The GNSS NavAer INCT project overview and main results. *Journal of Aerospace Technology and Management*, 14, e0722. https://doi.org/10.1590/jatm.v14.1249
- Moraes, A. O., Muella, M. T., de Paula, E. R., de Oliveira, C. B., Terra, W. P., Perrella, W. J., & Meibach-Rosa, P. R. (2018). Statistical evaluation of GLONASS amplitude scintillation over low latitudes in the Brazilian territory. Advances in Space Research, 61(7), 1776–1789. https://doi.org/10.1016/j.asr.2017.09.032
- Moraes, A. O., Vani, B. C., Costa, E., Abdu, M. A., de Paula, E. R., Sousasantos, J., et al. (2018). GPS availability and positioning issues when the signal paths are aligned with ionospheric plasma bubbles. GPS Solutions, 22(4), 95. https://doi.org/10.1007/s10291-018-0760-8
- Muella, M. T. A. H., de Paula, E. R., Kantor, I. J., Batista, I. S., Sobral, J. H. A., Abdu, M. A., et al. (2008). GPS L-band scintillations and ionospheric irregularity zonal drifts inferred at equatorial and low-latitude regions. *Journal of Atmospheric and Solar-Terrestrial Physics*, 70(10), 1261–1272. https://doi.org/10.1016/j.jastp.2008.03.013
- Muella, M. T. A. H., Duarte-Silva, M. H., Moraes, A. O., de Paula, E. R., de Rezende, L. F., Alfonsi, L., & Affonso, B. J. (2017). Climatology and modeling of ionospheric scintillations and irregularity zonal drifts at the equatorial anomaly crest region. *Annales Geophysicae*, 35(6), 1201–1218. https://doi.org/10.5194/angeo-35-1201-2017
- Olwendo, O. J., Baki, P., Cilliers, P. J., Doherty, P., & Radicella, S. (2016). Low latitude ionospheric scintillation and zonal plasma irregularity drifts climatology around the equatorial anomaly crest over Kenya. *Journal of Atmospheric and Solar-Terrestrial Physics*, 138–139(2), 9–22. https://doi.org/10.1016/j.jastp.2015.12.002

MORAES ET AL. 16 of 17

- Rino, C. L. (1979). A power law phase screen model for ionospheric scintillation: 1. Weak scatter. *Radio Science*, 14(6), 1135–1145. https://doi.org/10.1029/RS014i006p01135
- Rino, C. L. (2011). The theory of scintillation with applications in remote sensing. Wiley-IEEE Press. https://doi.org/10.1002/9781118010211
 Roddy, P. A., Hunton, D. E., Ballenthin, J. O., & Groves, K. M. (2010). Correlation of in situ measurements of plasma irregularities with ground-based scintillation observations. *Journal of Geophysical Research*, 115(A6), A06303. https://doi.org/10.1029/2010JA015288
- Salles, L. A., Vani, B. C., Moraes, A., Costa, E., & de Paula, E. R. (2021). Investigating ionospheric scintillation effects on multifrequency GPS signals. Surveys in Geophysics, 42(4), 999–1025. https://doi.org/10.1007/s10712-021-09643-7
- Shume, E. B., & Mannucci, A. J. (2013). First calculation of phase and coherence of longitudinally separated L-band equatorial ionospheric scintillation. Geophysical Research Letters, 40(14), 3496–3501. https://doi.org/10.1002/grl.50702
- Shume, E. B., Mannucci, A. J., Butala, M. D., Pi, X., & Valladares, C. E. (2013). Flux tube analysis of L-band ionospheric scintillation. *Journal of Geophysical Research: Space Physics*, 118(6), 3791–3804. https://doi.org/10.1002/jgra.50285
- Silva, A. L., Sousasantos, J., Marini-Pereira, L., Lourenço, L. F. D., Moraes, A. O., & Abdu, M. A. (2021). Evaluation of the dusk and early nighttime Total Electron Content modeling over the eastern Brazilian region during a solar maximum period. Advances in Space Research, 67(5), 1580–1598. https://doi.org/10.1016/j.asr.2020.12.015
- Sobral, J. H. A., Abdu, M. A., Takahashi, H., Taylor, M. J., de Paula, E. R., Zamlutti, C. J., et al. (2002). Ionospheric plasma bubble climatology over Brazil based on 22 years (1977–1998) of 630nm airglow observations. *Journal of Atmospheric and Solar-Terrestrial Physics*, 64(12–14), 1517–1524. https://doi.org/10.1016/S1364-6826(02)00089-5
- Sousasantos, J., Marini-Pereira, L., Moraes, A. O., & Pullen, S. (2021). Ground-based augmentation system operation in low latitudes-part 2: Space weather, ionospheric behavior and challenges. *Journal of Aerospace Technology and Management*, 13, e4821. https://doi.org/10.1590/iatm.v13.1237
- Sousasantos, J., Moraes, A. O., Di Santis, V., & Vani, B. C. (2024). Temporal characterization of pre-midnight fading events over low latitudes. Advances in Space Research, 73(1), 794–806. https://doi.org/10.1016/j.asr.2023.10.034
- Sousasantos, J., Moraes, A. O., Sobral, J. H. A., Muella, M. T. A. H., de Paula, E. R., & Paolini, R. S. (2018). Climatology of the scintillation onset over southern Brazil. *Annales Geophysicae*, 36(2), 565–576. https://doi.org/10.5194/angeo-36-565-2018
- Stolle, C., Lühr, H., & Fejer, B. G. (2008). Relation between the occurrence rate of ESF and the equatorial vertical plasma drift velocity at sunset derived from global observations. *Annales Geophysicae*, 26(12), 3979–3988. https://doi.org/10.5194/angeo-26-3979-2008
- Takahashi, H., Wrasse, C. M., Otsuka, Y., Ivo, A., Gomes, V., Paulino, I., et al. (2015). Plasma bubble monitoring by TEC map and 630 nm airglow image. *Journal of Atmospheric and Solar-Terrestrial Physics*, 130–131(8), 151–158. https://doi.org/10.1016/j.jastp.2015.06.003
- Vani, B. C., Forte, B., Monico, J. F. G., Skone, S., Shimabukuro, M. H., Moraes, A. O., et al. (2019). A novel approach to improve GNSS Precise Point Positioning during strong ionospheric scintillation: Theory and demonstration. *IEEE Transactions on Vehicular Technology*, 68(5), 4391–4403. https://doi.org/10.1109/TVT.2019.2903988
- Vani, B. C., Moraes, A. O., Salles, L. A., Breder, V. H. F., dos Santos Freitas, M. J., Monico, J. F. G., & de Paula, E. R. (2021). Monitoring ionospheric scintillations with GNSS in South America: Scope, results, and challenges. In GPS and GNSS technology in geosciences (pp. 255–280). Elsevier. https://doi.org/10.1016/B978-0-12-818617-6.00012-3
- Vargas, F., Brum, C., Terra, P., & Gobbi, D. (2020). Mean zonal drift velocities of plasma bubbles estimated from keograms of nightglow all-sky images from the Brazilian sector. Atmosphere, 11(1), 69. https://doi.org/10.3390/atmos11010069
- Whalen, J. A. (2000). An equatorial bubble: Its evolution observed in relation to bottomside spread F and to the Appleton anomaly. *Journal of Geophysical Research*, 105(A3), 5303–5315. https://doi.org/10.1029/1999JA900441
- Yeh, K. C., & Liu, C. H. (1982). Radio wave scintillations in the ionosphere. Proceedings of the IEEE, 70(4), 324–360. https://doi.org/10.1109/PROC.1982.12313
- Yokoyama, T. (2017). A review on the numerical simulation of equatorial plasma bubbles toward scintillation evaluation and forecasting. *Progress in Earth and Planetary Science*, 4(1), 37. https://doi.org/10.1186/s40645-017-0153-6

MORAES ET AL. 17 of 17